Investigation of the Lorentz gas in terms of periodic orbits

Predrag Cvitanović, Pierre Gaspard,[a] and Thomas Schreiber[b]
Niels Bohr Institute, Blegdamsvej 17, DK-2100 Copenhagen 0, Denmark

(Received 18 December 1991; accepted for publication 15 January 1992)

The diffusion constant and the Lyapunov exponent for the spatially periodic Lorentz gas are evaluated numerically in terms of periodic orbits. A symbolic description of the dynamics reduced to a fundamental domain is used to generate the shortest periodic orbits. Applied to a dilute Lorentz gas with finite horizon, the theory works well, but for the dense Lorentz gas the convergence is hampered by the strong pruning of the admissible orbits.

I. INTRODUCTION

The Lorentz gas[1] is one of the simplest nontrivial models of deterministic diffusion. Diffusion of a light molecule in a gas of heavy scatterers is modeled by a point particle in a plane bouncing off an array of reflecting disks. As a billiard built up completely of concave surfaces and as a pure hyperbolic system, the Lorentz gas is a good candidate for description in terms of cycle expansions.[2] This might seem a hopeless task, as one has to deal with all periodic and aperiodic solutions of an infinitely extended system. An approach based on larger and larger finite portions of the system is described in Ref. 3, with the diffusion constant related to the escape rates from such finite portions. As far as escape rates are obtained in direct numerical simulations this approach has been shown to be effective.[4] However, from the cyclists point of view where the rates are calculated from the periodic orbits, this approach is impractical; with each added disk new peculiarities arise in the enumeration of periodic orbits, and with current methods there is little hope of getting results for more than a few disks, and no hope of approaching the desired scaling limit.

A recent approach, introduced independently in Refs. 5 and 14 and tested in this paper, exploits the fact that the periodic Lorentz gas can be constructed by putting together translated copies of an elementary cell. Therefore quantities characterizing global dynamics, such as the Lyapunov exponent and the diffusion constant, can be computed from the dynamics restricted to the elementary cell.

II. THE PERIODIC LORENTZ GAS

In the periodic Lorentz gas[1] a point particle reflects elastically off a periodic array of reflecting disks in a plane. The system can be thought of as an unfolding of the Sinai billiard.[6] The standard diffusion constant can be defined if the particle has a bounded free path between any two successive bounces. An example is a triangular array with sufficiently small interdisk spacing. Unfortunately, as we shall see, the same mechanism that guarantees a finite horizon also leads to rather awkward pruning of periodic orbits.

Machta and Zwanzig[7] have given numerical results for the diffusion constant in Lorentz gases, as well as estimates based on a random walk approximation. We shall follow their notation and fix the radius of the disks to 1, assume unit particle speed, and denote the spacing between the disks by w (see Fig. 1). The horizon is finite for $w<4/\sqrt{3}-2=0.3094\ldots$.

III. DIFFUSION

In this section we briefly review the derivation of a formula for the diffusion coefficient of a spatially periodic system in terms of the periodic orbits in an elementary cell, originally given in Ref. 5 (which contains a more detailed treatment together with considerations about the discrete symmetries and a reduction of the dynamics to a fundamental domain).

The method applies to any hyperbolic dynamical system that is a periodic tiling $\widehat{M}=\cup_{\hat{n}\in T}M_{\hat{n}}$ of the dynamical phase space $\widehat{M}$ by translates $M_{\hat{n}}$ of an *elementary cell* M, with T the Abelian group of lattice translations.

It is convenient to define two time evolution operators, one for the whole phase space, and one for the elementary cell. Let $\hat{x}_t=\hat{\phi}(\hat{x})$ denote the point in the global space $\widehat{M}$ obtained by the flow in time t, and $x_t=\phi^t(x)$ denotes the corresponding flow in the elementary cell. The two are related by

$$\hat{n}_t(x)=\hat{\phi}^t(x)-\phi^t(x)\in T, \tag{1}$$

the translation of the endpoint of the global path into the elementary cell M.

Given a fixed vector $\beta\in\mathbf{R}^d$, where d is the dimension of the phase space, one can extract the diffusive properties of the Lorentz gas from the generating function

$$\langle e^{\beta\cdot(\hat{x}_t-x)}\rangle, \tag{2}$$

where the average is over all $x\in M$.

The diffusive properties follow by studying

$$Q(\beta)=\lim_{t\to\infty}\frac{1}{t}\log\langle e^{\beta\cdot(\hat{x}_t-x)}\rangle \tag{3}$$

[a]Permanent address: Université Libre de Bruxelles, Campus Plaine CP231, Blvd. du Triomphe, B-1050 Brussels, Belgium.

[b]Permanent address: Physics Department, University of Wuppertal, Gauss-Strasse 20, D-5600 Wuppertal 1, Germany.

 1054-1500/92/010085-06$001.00

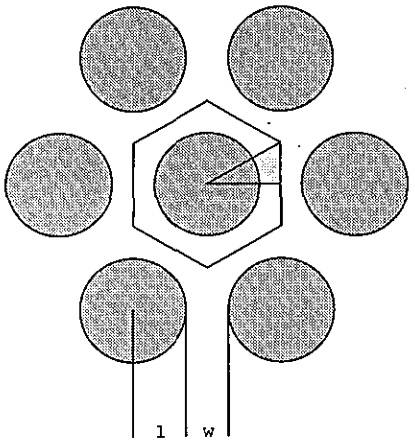

FIG. 1. A small portion of a triangular Lorentz gas. The whole set of scatterers can be obtained by translating the elementary cell indicated in the figure.

and its derivatives at $\beta = 0$. Clearly $Q(0) = 0$, and if by symmetry all odd derivatives vanish (i.e., there is no drift), the second derivatives

$$\frac{\partial}{\partial\beta_i}\frac{\partial}{\partial\beta_j} Q(\beta)\Big|_{\beta=0} = \lim_{t\to\infty} \frac{1}{t}\langle(\hat{x}_t - x)_i(\hat{x}_t - x)_j\rangle, \tag{4}$$

yield a (generically anisotropic) diffusion matrix. The spatial diffusion constant is then given by

$$D = \frac{1}{2\nu}\sum_{i=1}^{\nu} \frac{\partial^2}{\partial\beta^2 e} Q(\beta)\Big|_{\beta=0} = \lim_{t\to\infty} \frac{1}{2t}\langle(\hat{q}_t - q)^2\rangle, \tag{5}$$

where the i sum is restricted to the ν spatial components q_i of the phase space vectors x.

The basic ingredient of the approach is the reduction of the average (3) to the elementary cell. In order to understand this, recall that (3) can be written as

$$\langle e^{\beta\cdot(\hat{x}_t - x)}\rangle = \int_{\substack{x\in M\\ \hat{y}\in\hat{M}}} dx\, d\hat{y}\, e^{\beta\cdot(\hat{y}-x)}\,\mathrm{Prob}_t(x\to\hat{y}) \tag{6}$$

$$= \frac{1}{|M|}\int_{\substack{x\in M\\ \hat{y}\in\hat{M}}} dx d\hat{y}\, e^{\beta\cdot(\hat{y}-x)} \times\delta(\hat{y} - \hat{\phi}^t(x)). \tag{7}$$

Here, $|M| = \int_M dx$ is the volume of the elementary cell M. Note that there is a unique lattice translation $\hat{n}$ such that $\hat{y} = y - \hat{n}$, with $y\in M$. Now the translational invariance can be used to reduce the integral over y to the elementary cell:

$$\langle e^{\beta\cdot(\hat{x}_t - x)}\rangle = \frac{1}{|M|}\int_{x,y\in M} dx\, dy\, e^{\beta\cdot(\hat{\phi}^t(x) - x)} \times\delta(y - \phi^t(x)). \tag{8}$$

In this way the global $\hat{\phi}^t$ flow averages can be computed by following the flow ϕ^t restricted to the elementary cell M. As is well known,[8] the $t\to\infty$ limit of such averages can be recovered by means of transfer operators. Equation (8) suggests that we study the operator $\mathscr{L}^t$ whose kernel is given by

$$\mathscr{L}^t(y,\ x) = e^{\beta\cdot(\hat{x}_t - x)}\delta(y - x_t), \tag{9}$$

where $\hat{x}_t = \hat{\phi}^t(x)\in\hat{M}$, but $x, x_t, y\in M$. It is straightforward to check that this operator has the semigroup property,

$$\int_M dz\, \mathscr{L}^{t_2}(y,\ z)\mathscr{L}^{t_1}(z,\ x) = \mathscr{L}^{t_2+t_1}(y,\ x).$$

The quantity of interest (3) is given by the leading eigenvalue of $\mathscr{L}^t$, $\lambda_0 = e^{tQ(\beta)}$. In particular, for $\beta = 0$, the operator (9) is the Perron–Frobenius operator, with the leading eigenvalue $\lambda_0 = 1$ (the probability conservation).

To evaluate the spectrum of $\mathscr{L}$, consider

$$\mathrm{tr}\,\mathscr{L}^t = \int_M dx\, e^{\beta\cdot\hat{n}_t(x)}\delta(x - x_t). \tag{10}$$

Here $\hat{n}_t(x)$ is the discrete lattice translation defined in (1). For discrete time and hyperbolic dynamics we have

$$\mathrm{tr}\,\mathscr{L}^t = \sum_{\substack{p:\tau_p r = t,\\ r\in N}}\ \sum_{x\in p} \frac{e^{\beta\cdot\hat{n}_t(x)}}{|\det(\mathbf{1} - \mathbf{J}^r(x))|}, \tag{11}$$

where the sum is over periodic points of all prime cycles p whose period τ_p divides t, and $\mathbf{J}_p(x) = D\phi^{\tau_p}(x)$. Note that the sum over cycle points of p can be replaced by a factor τ_p, as $\det(\mathbf{1} - \mathbf{J}_p) = \det(\mathbf{1} - \mathbf{J}_p(x))$ and $\hat{n}_p = \hat{n}_{\tau_p}(x)$ are independent of x. For the Jacobian $\mathbf{J}_p$ this follows by the chain rule, and for the traveled distance $\hat{n}_p$ this follows by continuing the path periodically in $\hat{M}$. For the discrete time case we finally obtain

$$\det(1 - z\,\mathscr{L}) = \prod_p \exp\left(-\sum_{r=1}^{\infty}\frac{z^{\tau_p r}}{r}\frac{e^{r\beta\cdot\hat{n}_p}}{|\det(\mathbf{1} - \mathbf{J}_p^r)|}\right), \tag{12}$$

where the product runs over the set $\mathscr{P}$ of prime cycles.

Generalization to continuous time[9,10] amounts to the replacement $z^{\tau_p}\to e^{-s\tau_p}$, where τ_p is now the (not necessarily integer) period of the prime cycle p:

$$Z(\beta,s) = \prod_{p\in\mathscr{P}} \exp\left(-\sum_{r=1}^{\infty}\frac{1}{r}\frac{e^{(\beta\cdot\hat{n}_p - s\tau_p)r}}{|\det(\mathbf{1} - \mathbf{J}_p^r)|}\right). \tag{13}$$

The associated Ruelle zeta function is then (see, e.g., Ref. 2 for details)

$$\frac{1}{\zeta(\beta,s)} = \prod_{p\in\mathscr{P}}\left(1 - \frac{e^{\beta\cdot\hat{n}_p - s\tau_p}}{|\Lambda_p|}\right), \tag{14}$$

with $\Lambda_p = \prod_e \lambda_{p,e}$ the product of the expanding eigenvalues of $\mathbf{J}_p$.

The first main result of Ref. 5 is that the function $Q(\beta)$ of Eq. (3) is the largest solution of the equation $Z(\beta,Q(\beta)) = 0$ [or equivalently, of $1/\zeta(\beta,Q(\beta)) = 0$].

The above infinite products can be rearranged as expansions with improved convergence properties.[2] To present the result, we define $t_p = e^{\beta\cdot\hat{n}_p - s\tau_p}/|\Lambda_p|$, and expand the zeta function (14) as a formal power series,

$$\prod_{p\in\mathcal{P}}(1-t_p)=1+\sum_{p_1,\ldots,p_k}{}' t_{\{p_1,\ldots,p_k\}}, \tag{15}$$

where

$$t_{\{p_1,\ldots,p_k\}}=(-1)^k t_{p_1}t_{p_2}\cdots t_{p_k}, \tag{16}$$

and the sum is over all distinct nonrepeating combinations of prime cycles. Taking two derivatives, as in the derivation of Eq. (35) and Eq. (80) in Ref. 2 one obtains the main formula tested numerically in this paper.

The diffusion constant (5) is given by

$$D=\frac{1}{2\nu}\frac{\Sigma'(-1)^k(\hat{n}_{p_1}+\cdots+\hat{n}_{p_k})^2/|\Lambda_{p_1}\cdots\Lambda_{p_k}|}{\Sigma'(-1)^k(\tau_{p_1}+\cdots+\tau_{p_k})/|\Lambda_{p_1}\cdots\Lambda_{p_k}|}, \tag{17}$$

with sums as in (15). The beauty of this formula is that even though the global trajectory is in general not periodic, $\hat{n}_p\neq 0$, the reduction to the elementary cell enables us to compute the desired quantity in the usual way in terms of periodic orbits.

Apart from the diffusion constant we will compute Lyapunov exponents and test the probability conservation. Because it involves derivatives of zeta functions the formula for the largest Lyapunov exponent takes a similar form as the one for the diffusion constant above (17). The formula (modified for continuous time) is given in Ref. 2, Eq. (91):

$$\lambda=\frac{\Sigma'(-1)^k(\mu_{p_1}+\cdots+\mu_{p_k})/|\Lambda_{p_1}\cdots\Lambda_{p_k}|}{\Sigma'(-1)^k(\tau_{p_1}+\cdots+\tau_{p_k})/|\Lambda_{p_1}\cdots\Lambda_{p_k}|}. \tag{18}$$

In this formula $\mu_p=\ln|\Lambda_p|$ denotes the stability of a cycle. Note that all quantities involved here are invariant under the symmetries of the lattice.

A. A simple example: A chain of baker's maps

Some confidence can be gained at this point by applying the above formula (17) to a trivial system, a chain of coupled baker maps studied in Ref. 11. In this case there are only four fixed points, all with stability $\Lambda_p=1/2$, two of which give rise to the translations $\hat{n}_p=\pm 1$. As the system is uniformly hyperbolic, all curvature terms are identically zero, and the fixed points substituted into (17) yield immediately the correct result $D=1/4$.

IV. DYNAMICS IN THE ELEMENTARY CELL

Unfolding a periodic orbit in the elementary cell can result in a closed orbit in the whole lattice or in a segment of some translational movement. According to the above result (17) the diffusive properties of the system follow from the relation between the closed and the translating orbits.

Since the system is closed the escape rate is zero. Therefore the dynamical zeta function [Eq. (14) with $\beta=0$] should have its first zero at $z=1$. $\zeta(0,0)$ is simply $1+\Sigma'(-1)^k/|\Lambda_{p_1}\cdots\Lambda_{p_k}|$.

The periodic orbits in the elementary cell can be found in a systematic way. Starting at a given disk, the trajectory can reach any of the neighboring 12 disks in the next bounce. A symbolic dynamics is obtained by labeling these displacements anticlockwise with numbers 0 to 11. When 0 denotes a flight between disks which are nearest neighbors all even numbers do so. For any spacing there is an obvious pruning rule that motion in the same direction cannot be repeated twice in a row because the particle cannot cross a disk. In fact, for the dense gas considered here, the direction has to change at least by two units after each bounce. After a long flight (odd label) the change has to be at least 3.

TABLE I. Elementary cell, $w=0.3$.

Length	# cycles	$\zeta(0,0)$	λ	D
1	0	...	...	...
2	24	−0.31697	1.330	0.750
3	64	−0.54152	1.435	0.677
4	156	−0.09718	1.902	0.565
5	492	0.02383	2.324	0.425
6	1484	0.02812	1.931	0.259
7	5244	0.02044	1.836	0.371
8	19008	−0.00036	1.754	0.513
Ref. 7, estimate				0.175
Numerical experiment				0.25

The cycles corresponding to a given sequence can now be found, e.g., by minimizing the length of a path visiting the disks according to the symbols.

Although the discrete C_{6v} symmetry of the elementary cell is not exploited in the diffusion formula, it can be used to reduce the necessary computational effort. The images of a cycle under rotation and reflection do not have to be computed separately. Nevertheless the huge number of

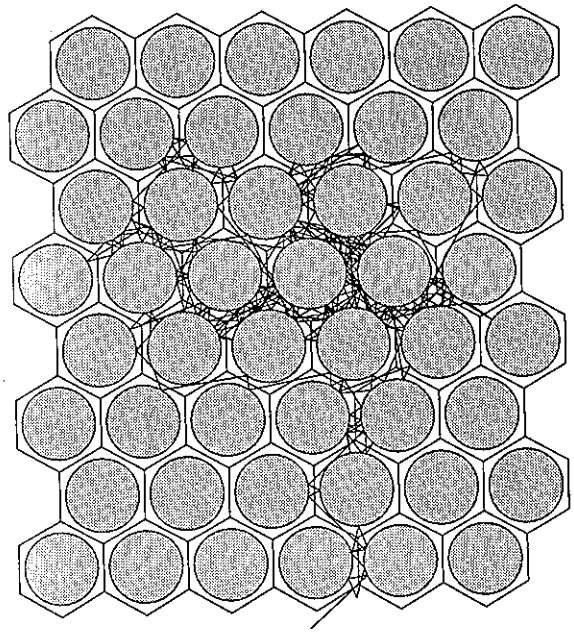

FIG. 2. A portion of a chaotic trajectory with about 300 bounces is shown. Although the particle is often trapped between neighboring disks for several bounces, there are also segment of the trajectory which take the particle over a large distance with few bounces.

TABLE II. Elementary cell, $w = 2.0$, imposed finite horizon.

Length	# cycles	λ	D
1	0	...	...
2	54	0.5528	1.6716
3	440	0.5588	1.7006
4	3234	0.5604	1.7054
5	27856	0.5605	1.7049

symbols drastically restricts the maximal cycle length attainable in numerical calculations.

Table I shows the results obtained for a spacing of $w = 0.3$. Note that because of the pruning rule there cannot be a fixed point with these symbols.

As mentioned above a lot of orbits turn out to be forbidden when the required finite horizon is achieved by making the spacing between disks small enough. This is immediately reflected in the fact that the number of orbits does not increase by a factor of 11 each time the length is increased. Indeed, for the cycles computed so far, the average factor is less than 4. So very poor convergence of cycle expansions has to be expected. With this in mind the numbers given in Table I are in a reasonable accord with the probability conservation and also not a disaster for the Lyapunov exponent (compare with the more accurate estimates of Table V). Nevertheless, the estimates of the diffusion constant up to the number of cycles employed so far do not show any convergence at all. They seem to be more sensitive to the bad shadowing than the Lyapunov exponent and the probability conservation.

A. Dilute Lorentz gas

In order to test the diffusion formula under less trying conditions, we eliminate pruning by making the spacing between disks larger, and imposing the finite horizon by fiat; in this section we consider the measure zero subset of those orbits which after each bounce travel only to one of the nearest or next-nearest disks (see Fig. 2). This set is a Cantor set repeller, and the probability is not conserved. Estimates of the Lyapunov exponent and the diffusion constant for trajectories restricted to this set are given in Table II.

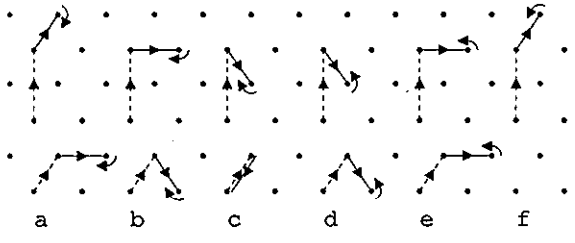

FIG. 3. The upper row shows the case when the preceding segment has been a long one, the lower row the case when it has been a short one. The arrows at the end points indicate the sense of the next change of direction. Due to the discrete symmetry of the triangular lattice, all translated, rotated or reflected copies of each situation shown are denoted by the same symbol.

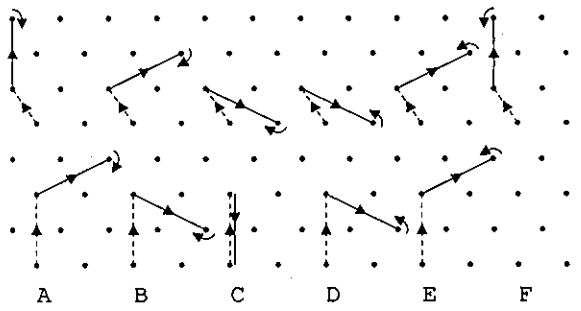

FIG. 4. The upper row shows the case when the preceding segment has been a short one, the lower row the case when it has been a long one.

As the set is not the full set of orbits contributing to diffusion, there are no results obtained by other means that these numbers could be compared with. Encouragingly, the diffusion constant exhibits reasonable convergence, supporting the claim that the cycle expansion formula is in principle convergent, but for high density of scatterers the convergence is adversely affected by the strong pruning of the allowed orbits.

V. REDUCTION TO THE FUNDAMENTAL DOMAIN

In Ref. 5 some effort is made to derive a diffusion formula similar to (17) involving quantities within the fundamental domain. The fact that lattice translations do not commute with the symmetry group within the elementary cell makes this apparently a difficult and not yet completed task. Therefore only results for the Lyapunov exponent (18) and the probability conservation are given in this section.

The fundamental domain dynamics used here, due to F. Christiansen,[12] is given in Figs. 3, 4, and Table III. Now the symbols indicate relative direction changes instead of the absolute directions. The right and left turns are not distinguished—instead, one reads off a symbol whether the next turn has to be taken in the same or in the opposite sense. Lower case letters denote short flights between closeby disks, upper case letters denote the long flights to

TABLE III. Symbols in the fundamental domain.

	Amount of change		Direction of change	
Symbol	Last long	Last short	Next the same	Next other way
a	1	2	x	
b	3	4	x	
c	5	6	x	
d	5	4		x
e	3	2		x
f	1	...		x
A	2	1	x	
B	4	3	x	
C	6	5	x	
D	4	5		x
E	2	3		x
F	-	1		x

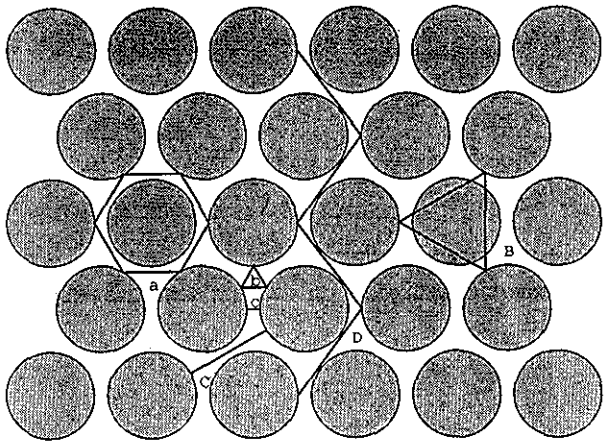

FIG. 5. Shown are global orbits which reduce to fixed points in the fundamental domain. Five of them (a,b,c,C,D) are not pruned for $w = 0.3$, the spacing shown here. The sixth (B) is an example of a pruned cycle; it exists for a dilute Lorentz gas, but for the dense Lorentz gas its trajectory is blocked by the center disk. Both B and D denote turns by 120 deg, but D also changes the sense of rotation at each bounce.

the next nearest disks. Each symbol corresponds to a given relative change in direction. The exact amount of change depends on whether the last flight was long (odd label in the notation of the last section) or short (even label).

Christiansen[12] had originally proposed to denote symbols "f" and "F" by the same letter, thus reducing the size of the alphabet. We prefer to use instead the two letters together with the pruning rule that "f" can only follow an uppercase letter (i.e., a long segment) and "F" only a lowercase letter. The symbols given to an orbit by this scheme are invariant under all spatial symmetries of the system but not under the time reversal.

Of the possible 12 symbols, "A," "B," "f," and "F" are pruned as soon as the horizon gets finite. Among the remaining symbols there is still strong pruning, reflected in the fact that for $w = 0.3$ the number of cycles of symbol length n does not grow like 8^n but roughly as 3^n. Figure 5 shows all the fundamental domain fixed points which are not pruned at $w = 0.3$ together with an example of a pruned fixed point.

Table IV gives some impression of the pruning involved. In order that longer orbits be shadowed by shorter ones, for every combination of two symbols a two-cycle,

TABLE IV. Problematic shadowing, $w = 0.3$.

		a	b	c	d	e	C	D	E
	1	x	x	x			x	x	
a	x	⋯	x		x				
b	x	x	⋯	x	x	x			x
c	x		x	⋯	x	x		x	
d		x	x	x	⋯			x	
e			x	x		⋯			
C	x						⋯		
D	x			x	x			⋯	
E			x						⋯

TABLE V. Fundamental domain, $w = 0.3$.

Length	# cycles	$\zeta(0,0)$	λ
1	5	− 1.216 975	⋯
2	10	− 0.024 823	1.745 407
3	32	− 0.021 694	1.719 617
4	104	0.000 329	1.743 494
5	351	0.002 527	1.760 581
6	1243	0.000 034	1.756 546

and the fixed points corresponding to each of the symbols should exist. Two-cycles such as "ac," "aC,"...are missing while corresponding "shadowing" pseudo-cycles "ac," "aC" exist, and conversely, two-cycles occur where one of the symbols has no corresponding fixed point (e.g., the symbol "d" in "ad"). So shadowing seems to be largely disfunctional, at least as long as finite approximate Markov partitions[15] are not developed. With this in mind the convergence which can be seen in Table V is better than expected. Furthermore, for general reasons discussed in Ref. 13, the convergence of cycle expansions for dynamics restricted to the fundamental domain is considerably better than for the elementary cell, as can be verified by comparing the Lyapunov exponent and probability conservation estimates in the two cases.

To conclude, we have tested numerically the recently proposed formula for deterministic diffusion in the Lorentz gas. While the cycle expansions work well in estimating the more traditional indicators of deterministic chaos, such as the Lyapunov exponent, they do not yet lead to converging estimates of the diffusion constant for the dense Lorentz gas. This appears to be a consequence of the severe symbolic dynamics pruning and the attendant lack of shadowing in cycle expansions. Whether this difficulty can be surmounted by more careful control of the symbolic dynamics remains to be seen.

ACKNOWLEDGMENTS

PC is grateful to the Carlsberg Foundation for support. TS receives a grant within the framework of the SCIENCE programme of the Commission of the European Communities under contract no B/SC1*-900557. PG is "Chercheur Qualifié" at the National Fund for Scientific Research (Belgium) and is grateful to Nordita and NATO for support during the "Quantum Chaos and Measurement" workshop, Copenhagen, Spring 1991.

[1] H. A. Lorentz, Proc. Amst. Acad. 7, 438 (1905).
[2] R. Artuso, E. Aurell, and P. Cvitanović, Nonlinearity 3, 325 (1990).
[3] P. Gaspard and G. Nicolis, "Transport properties, Lyapunov exponents, and entropy per unit time," Phys. Rev. Lett. 65, 1693 (1990).
[4] P. Gaspard and F. Baras, "Dynamical Chaos underlying Diffusion in the Lorentz Gas," in *Microscopic Simulations of Complex Hydrodynamic Phenomena*, NATO ASI, Alghero, Sardinia, 15–27 July 1991, edited by M. Maréschal and B. L. Holian (Plenum, London, 1991).
[5] P. Cvitanović, J.-P. Eckmann, and P. Gaspard, "Transport Properties of the Lorentz Gas in Terms of Periodic Orbits," Niels Bohr Institute preprint (May 1991).
[6] Ya.G. Sinai, Usp. Mat. Nauk 25, 141 (1970).

[7] J. Machta and R. Zwanzig, "Diffusion in a periodic Lorentz gas," Phys. Rev. Lett. **50**, 1959 (1983).
[8] D. Ruelle, *Statistical Mechanics, Thermodynamic Formalism* (Addison-Wesley, Reading MA, 1978).
[9] R. Bowen, *Equilibrium States and the Ergodic Theory of Anosov-diffeomorphisms,* Springer Lecture Notes in Mathematics, Vol. 470 (Springer-Verlag, Berlin, 1975).
[10] P. Cvitanović and B. Eckhardt, "Periodic orbit expansions for classical smooth flows," J. Phys. A **24**, L237 (1991).
[11] P. Gaspard, "Diffusion, Effusion and Chaotic Scattering: An Exactly Solvable Liouvillian Dynamics," Brussels preprint (1990).
[12] F. Christiansen (private communication).
[13] P. Cvitanović and B. Eckhardt, "Symmetry decomposition of chaotic dynamics," submitted to Nonlinearity.
[14] R. Artuso, "Diffusive dynamics and periodic orbits of dynamical systems," Phys. Lett. A (in press).
[15] L. Bunimovich and Ya. G. Sinai, "Markov Partition for Dispersed Billiard," Commun. Math. Phys. **78**, 247 (1980); **78**, 479 (1980) Erratum, **107**, 357 (1986).